POLDER-2 / Ocean Color

ATBD
Atmospheric correction Algorithms

Version 1.1, october 2005

J.-M. Nicolas, P.-Y. Deschamps, H. Loisel, C. Moulin

Table of contents

Atmospheric correction

The purpose of atmospheric corrections is to remove the atmospheric contribution, whether absorbing or scattering ones, from the signal measured by the satellite. Over ocean, that contribution is very significative, from 70 to more than 90 % of the Top Of the Atmosphere signal. The objectives of that document is to describe the modelisation used and the algorithm developped to carry off atmospheric corrections for POLDER-2 instruments. The level of description should be helpful for scientist users but is by no way an operationnal specification.

Radiometric model

POLDER level-1 data are normalized radiances, defined for each band as :

$$R(\lambda) = \pi.L(\lambda)/F_0(\lambda) \qquad (1)$$

Where $L(\lambda)$ is the radiances corrected from sun-earth distance and $F_0(\lambda)$ is the extra-terrestrial solar irradiance.

That Top-Of-Atmosphere (TOA) normalized radiance is then decomposed as :

$$R = T_{O3,O2}\left[R_{atm} + T_{H2O}\left\{t.R_g + \frac{\mu_s.T^{\downarrow\uparrow}.\rho_s}{1 - S.\rho_s}\right\}\right] + R_{strato} \qquad (2)$$

Where T_{O3}, T_{O2}, T_{H2O} account for gaseous absorption by ozone, oxygen and water vapour respectively, R_{strato} accounts for stratospheric aerosols contribution, R_{atm} accounts for troposphere (molecules + aerosols) contribution and the term between brackets (detailed below) account for surface (sun-glint, water and foam reflectance) contributions. The dependence on wavelength has been omitted to simplify writing.

Gaseous absorption and stratospheric aerosols corrections are made just after clouds masking and before any atmospheric corrections (figure xx, organigram 1). The corrected signal can then be decomposed as :

$$R^1(\lambda) = R_{mol}(\lambda) + R_{gm}(\lambda) + R_a(\lambda) + t(\lambda).R_g + \frac{\mu_s.T^{\downarrow\uparrow}(\lambda).[\rho_w(\lambda) + \rho_f(\lambda)]}{1 - S(\lambda).[\rho_w(\lambda) + \rho_f(\lambda)]} \qquad (3)$$

Where :

$R_{mol}(\lambda)$ accounts for multiple scatterings by molecules

$R_{gm}(\lambda)$ accounts for coupling terms between molecules and photons reflected on a rough sea surface ; all Look Up Tables (LUT) are computed for a wind speed of 2 m/s (as defined for an isotropic Cox and Munk model) so that term is 0 for a surface wind speed of 2 m/s, and different from 0 for other wind speed.

$R_a(\lambda)$ accounts for multiple scatterings by aerosols and by (molecules+aerosols). In order to include multiple scattering on both molecules and aerosols (coupling), that term is computed as $R_a(\lambda) = R_{tot}(\lambda) - R_{mol}(\lambda)$, where $R_{tot}(\lambda)$ is the total (aerosols+molecules) scattering term and $R_{mol}(\lambda)$ is the scattering term by molecules as already defined. That decomposition allows to adjust the molecular term by sea-surface pressure without modifying the aerosol term.

$t(\lambda).R_g$ accounts for direct sun-glint ; $t(\lambda)$ is the direct transmittance of the atmosphere, defined by :

$t(\lambda) = \exp[-(\tau_r(\lambda) + \tau_a(\lambda))*(1/\mu_s + 1/\mu_v)]$ where τ_r and τ_a are respectively the molecules and aerosols optical thickness and μ_s and μ_v are the cosines of solar and viewing zenith angles respectively. R_g is the sun-glint reflectance as modelled by (Cox and Munk , 1954) (§ *glitter mask*)

$T^{\downarrow\uparrow}(\lambda)$ is the total (direct + diffuse) downward and upward transmission by the atmosphere (molecules + aerosols)

$S(\lambda)$ is the spherical albedo of the atmosphere

$\rho_w(\lambda)$ and $\rho_f(\lambda)$ are the water reflectance and the foam reflectance respectively

Conditions of the simulations

The radiative transfer equation in the ocean-atmosphere system is solved using a Successive Order of Scattering (SOS) code including polarisation and a rough sea surface (Deuzé et al, 1989). The LUT described below are all computed using that code with 24 gauss nodes for solar and zenith angles and 37 nodes (each 5°) for azimuth angles.

Depolarisation factor of atmosphere molecules has been set to 0.0279 (Young, 1980). Rayleigh optical thickness for each band has been weighted by the solar irradiance and the band spectral response function:

$$\langle \tau_r(\lambda) \rangle = \frac{\int \tau_r(\lambda).F_0(\lambda).SR(\lambda).d\lambda}{\int F_0(\lambda).SR(\lambda).d\lambda}$$

Where $F_0(\lambda)$ is the extraterrestrial solar irradiance, $SR(\lambda)$ is the band spectral response function and $\tau_r(\lambda)$ is the atmospheric rayleigh optical thickness for wavelength λ. $\tau_r(\lambda)$ is computed using fitting equation proposed by (Hansen and Travis, 1974), lowered by 0.53 % to take into account our choice of a depolarisation factor of 0.0279 instead of their value of 0.031. That equation is :

$$\tau_r(\lambda) = 0.008524\lambda^{-4} (1 + 0.0113\lambda^{-2} + 0.00013\lambda^{-4}) \quad (4)$$

$<\tau_r(\lambda)>$ used in computation of LUT are given in table 1.

The atmosphere is decomposed in 26 vertical layers with different aerosols-molecules mixing ratios for each. Vertical profile of aerosols is supposed to be exponential with the altitude :

$$\tau_{tot} = \tau_a.\exp(-z/H_a) + \tau_r.\exp(-z/H_r)$$

where z is the altitude of the top of the layer, τ_a and τ_r are the aerosol and molecular optical thickness respectively, H_a and H_r are set to 2 km and 8 km respectively.

Transmittance considerations

Total transmittance (i.e. direct + diffuse) and spherical albedo of the atmosphere are computed exactly using SOS code. The conditions of the simulation are the one described above (rough sea surface, no diffuse contribution of the ocean). Total transmission, whether downward or upward, for a given zenith angle is given by:

$$T(\lambda,\theta) = \exp(-\frac{\tau_r + \tau_a)}{\cos(\theta)}) + E(\lambda,\theta)$$

where $E(\lambda,\theta)$ is the diffuse transmittance of the atmosphere, τ_r and τ_a are the rayleigh and aerosol optical thickness respectively and θ is the solar or viewing zenith angle :

$$T^{\downarrow\uparrow}(\lambda) = T^{\downarrow}(\lambda).T^{\uparrow}(\lambda) = T(\lambda,\theta_s).T(\lambda,\theta_v)$$

The spherical albedo of the atmosphere $S(\lambda)$ accounts for successive photons interactions with surface, then atmosphere and surface again. For Ocean Color applications, where surface reflectance is generally small compared to atmospheric scattering, those contributions are small. It is given by :

$$S(\lambda) = 2\pi.\int_0^1 E_{up}(\lambda,\mu)\mu.d\mu$$

Where $\mu = \cos(\theta)$, and $E_{up}(\lambda,\theta)$ is the diffuse upward irradiance of the atmosphere for a solar zenith angle of θ. Because our simulation code (SOS) use Gauss polynomial decomposition for geometric conditions, $S(\lambda)$ can be exactly computed using Gauss nodes and weight :

$$S(\lambda) = 2.\sum_{i=1}^{N_{gauss}} E_{up}(i).Ga(i).\mu(i)$$

Where Ga(i) and μ(i) account for the Gauss weight and cosinus Gauss angle of Gauss node i. In our simulations, N_{gauss}=24.

Correction for sea surface pressure variations

In order to correct for sea surface pressure variations, the term accounting for multiple scatterings by molecules $R_{mol}(\lambda)$ is corrected following $R_{mol}(\lambda)= R_{mol}(\lambda)\ P/P_0$. In the same way the total transmission has been decomposed as $T_{tot}(\lambda)=T_m^-(\lambda).T_a^-(\lambda).T_m^+(\lambda).T_a^+(\lambda)$, where – and + account for downward and upward transmittance respectively and m and a account for molecular and aerosol transmittance, respectively. Molecular transmittance is then corrected from surface pressure variations using $(1-T_m)=(P_0/P).(1-T_m)$. P is the sea surface pressure and P_0=1013 hPa is the standard conditions pressure.

Precisions of the radiometric model

It should be noticed that no approximated formulae have been used. The decomposition of eq. (3) is exact under the following hypothesis :

- surface reflectance above the air-sea interface is supposed lambertian
- multiple interaction between sea water, then atmosphere, then air-sea surface (fresnel reflection) then atmosphere again are supposed negligible.

Glitter mask

Some directions of the multi-angular view of a same pixel are filtered to reject sun glint contamination. It must be noted that in many cases, each pixel has some viewing direction out of that sun-glint, hence the satellite coverage is almost not affected by sun-glint.

Still, directions contaminated by sun-glint should be discarded. For each pixel and each direction, sun-glint reflectance for a surface wind speed u is given by :

$$R_g(\theta_S,\theta_V,\varphi,u) = \frac{\pi.P(Z(u)).R_{fresnel}(\gamma)}{4.\cos^4(\beta).\mu_S} \qquad (5)$$

Where $R_{fresnel}$ is the reflection coefficient at the air-sea interface for the scattering angle γ, β is the wave inclination and P(Z(u)) is the gaussian slope distribution as given by Cox and Munk. Surface wind speed comes from ancillary data. If R_g is greater than a threshold value R_{g_lim} then the viewing direction is discarded. For POLDER processing #1,2 and 3, R_{g_lim} has been set to 0.005. If the direction is not discarded ($R_g < R_{g\_lim}$), the computed R_g value is used in the atmospheric correction scheme for sun-glint correction (eq. 3).

Description of the atmospheric correction algorithm

The general idea of the algorithm is well-known : to use spectral bands where ocean surface reflectance is very low to assess aerosol quantities (optical thickness) and qualities (angström coefficient and model). Those information's are then extrapolated to ocean colour bands in order to correct the signal from atmospheric perturbations. As in (Gordon and Wang , 1994), aerosol inversion relies on models developed by (Shettle and Fenn, 1979). This set of models is detailed in table 2 and figures 1,2 and 3.

In addition, the POLDER-2 algorithm includes some new important including :

- an new way to deal with the so-called "black pixel assumption" for atmospheric correction over eutrophic or case-2 waters where marine reflectance in the red cannot be neglected
- an original new atmospheric correction for absorbing aerosol based on POLDER directionnal information.

The core of the algorithm is a two-steps process with one iteration (organigram 2.). In a first step, the aerosol model is computed for a given optical thickness. In a second step, the optical thickness is computed for the model inverted in step 1. Because of the multiple scattering effects, those two steps are played twice. Then, atmospheric correction of Ocean Colour bands is carried on using the aerosol model and optical thickness inverted. Specific operations have been implemented for sun-glint and foam correction and will be detailed below.

In order to deal with absorbing aerosols, we have defined some kind of *aerosols families*, from non-absorbing aerosol family to highly absorbing one. The idea is to play the core of the algorithm for each family (one family is made of 12 aerosol models), and then to choose the very family that best fit directional observations.

That algorithm heavily relies on exact simulation of the TOA radiances for each pixel and viewing directions and for multiple geophysical conditions. Those simulations are CPU-consuming and are incompatible with global dataset processing. For that reason Look-Up Tables are beforehand computed. The simulations really used in the algorithm are then linearly interpolated on multiple variables (solar and viewing angles, aerosol models, optical thickness).

Solar zenith angle, view zenith angle and relative azimuth angle are available for each pixel and each viewing direction in level-1 product. That is enough precision for solar zenith angle (there is a lapse of about four minutes between the first and the last sequence for an observed spot on earth). But for view zenith angle and relative azimuth angle a fine geometric registration correction for each band is computed to account for the small lapse of 0.306 second between measurements in two different bands. Each measurements are then associated to a geometry exactly defined by a triplet $[\theta_s(i), \theta_v(\lambda_j,i), \phi(\lambda_j,i)]$ where λ_j is the wavelength of band j and i is the indice of viewing direction.

Aerosol model inversion

The first step of the process is the evaluation of the spectral dependence of the observed aerosol in the red and Near-Infra-Red (NIR) part of the spectrum and then of the model that can be associated with that spectral dependence, including multiple scattering effects. First, the corrected normalised radiance (R_{corr}) is computed from the TOA normalised radiance as measured by the instrument for each band (j=670, 765, 865) and each viewing direction i :

$$R_{corr}(\lambda_j,i) = R_{mes}(\lambda_j,i) - R_{mol}(\lambda_j,i) - R_{gm}(\lambda_j,i) - t(\lambda_j,i).R_g - \frac{\mu_s.T^{\downarrow\uparrow}(\lambda_j,i).\rho_f(\lambda_j)}{1 - S(\lambda_j).\rho_f(\lambda_j)} \qquad (6)$$

Then the weighted spectral dependence measured over all viewing directions is computed :

$$\varepsilon = \sum_i \frac{A.R_{corr}(670,i) + (1-A).R_{corr}(765,i)}{R_{corr}(865,i)} \qquad (7a)$$

and for each aerosol model available in our LUT database the same computation is carried on :

$$\varepsilon_{\text{mod}} = \sum_i \frac{A.R_{\text{mod}}(670,i) + (1-A).R_{\text{mod}}(765,i)}{R_{\text{mod}}(865,i)} \tag{7b}$$

where $R_{\text{mod}}(\lambda_j, i)$ is linearly interpolated on four variables (θ_s, θ_v, ϕ, τ_a) in pre-computed LUT. The variable A is set between 0 and 1. For POLDER-1 algorithm, A has been set to 1 because the noise affecting the bands 763 and 765 is too high and would strongly affects the retrieved marine reflectance.

Two models x and y are then chosen in order that $\varepsilon_x < \varepsilon < \varepsilon_y$ The distance dis-x is also computed :

$$dis - x = \frac{\varepsilon - \varepsilon_x}{\varepsilon_y - \varepsilon_x} \tag{8}$$

Our 12 models have been organised in growing ε_{mod} orders and selected so that their ε_{mod} never cross each other for the geometries generally observed (figure 2.). The model that best fit the observation is then coded on a real number between 1 and 12 :

Xdis-X = x + dis-x (9)

A specific procedure has been developed for very clear observations : in that case, the spectral dependence is highly unpredictable because the denominator in equation 7 is very small. In order not to add noise in the final paramaters (marine reflectance and chlorophyll concentration), it has been decided to forced the model to a fixed value (C90) for very low aerosol charges. A threshold is applied on R_{corr} for each direction, and when a direction is below the threshold, its spectral dependence is forced to the value of the fixed model. For POLDER-1 the threshold accounts for an aerosol optical thickness of about 0.05.

Dealing with the "black pixel assumption"

Aerosol model inversion rely on the hypothesis of black ocean from 865 to 670 nm. It is now demonstrated that it is not true over eutrophic and case-2 waters where absorption of pure water is counterbalanced by the diffusion by particles (organic or inorganic). Thus the contribution of marine reflectance leads generaly to overestimate aerosol angström coefficient. The computation of the marine reflectance is necessary prior to aerosol inversion, which in turn is necessary to correctly compute marine reflectance… Solutions currently developped rely on iterative process (Siegel et al, 2000) or on spatial homogeneity of aerosols versus water heterogeneity (Ruddick et al, 2000).

For POLDER-2 operational algorithm, where computation time should be minimised, a simpliest solution has been developped, based on empirical relationship between marine reflectance at 565 and 670 nm (figure 4). That solution, first developped for CZCS algorithm by (Viollier et al., 1984), has shown to work reasonnably well for waters that can be observed at POLDER spatial resolution, including high sedimentation and coccolithophorus bloom situations. Problems potentially arise over waters highly charged with yellow substances where POLDER-2 algorithm will not work correctly.

The hypothesis is that a linear relationship exists between marine reflectance at 565 and 670 :

$\rho_w670 = a.\rho_w565 + b$
where a ~ 0.20 and b ~ -0.0005

using that relation, a rough approach can be to compute a new weighted spectral dependence defined as :

$$\varepsilon = \sum_i \frac{A.[R_{corr}(670,i) - a.R_{corr}(565,i) + b] + (1-A).R_{corr}(765,i)}{R_{corr}(865,i)} \tag{10}$$

where marine contribution at 565 and 670 cancel each other.

Optical thickness inversion

The second step of the process is the inversion of the aerosol optical thickness from observations. We used for that R_{corr} at 865 nm for all viewing directions. For each of them and each tabulated optical thickness (table 3) the value $R_{\mathrm{mod}}(865, i, \tau_a)$ is interpolated on four variables (θ_s, θ_v, ϕ, X-disX) in pre-computed LUT. Arithmetic mean over all viewing directions is then computed for R_{mod} and R_{corr} and the aerosol optical thickness τ_a is then given by :

$$\tau_a = \frac{\left[\left\langle R_{\mathrm{mod}}(865, \tau_a^2\right\rangle - \left\langle R_{corr}(865)\right\rangle\right]\tau_a^1 + \left[\left\langle R_{corr}(865)\right\rangle - \left\langle R_{\mathrm{mod}}(865, \tau_a^1\right\rangle\right]\tau_a^2}{\left\langle R_{\mathrm{mod}}(865, \tau_a^2\right\rangle - \left\langle R_{\mathrm{mod}}(865, \tau_a^1\right\rangle} \qquad (11)$$

where $\left\langle R_{\mathrm{mod}}(865, \tau_a^1\right\rangle$ and $\left\langle R_{\mathrm{mod}}(865, \tau_a^2\right\rangle$ are the simulated radiances for aerosol model X-disX evaluated above and for tabulated aerosol optical thickness τ_a^1 and τ_a^2 respectively that surround the corrected radiance (i.e. from instrument measurements) $\left\langle R_{corr}(865)\right\rangle$.

Dealing with absorbing aerosol

Absorption by aerosols is a difficult problem to solve because its main impact is observed in the very bands used for Ocean Color applications, i.e. for short wavelengths, because rayleigh scattering is maximum for these wavelength, and the absorption affect is proportional to the level of the signal. Near Infra Red information cannot be extrapolated in the visible part of the spectrum. One solution developed by (Gordon et al 1997) is to considered that atmospheric corrections needs to use simultaneously all the bands available and to distinguish between atmospheric and ocean effects using the differences between their respective spectral signature. That so-called spectral matching algorithm works reasonably well (Moulin et al, 2001) for sensors with at least six bands in the visible, from 412 to 670n nm, including 510 or 520 nm).

A new approach using the multi-directionality of POLDER has been developed to deal with such absorbing aerosols. It relies on the change of absorption efficacy with molecular scattering and air mass changes. We have plotted on the figure 5 the directional marine reflectances for a POLDER pixel above an absorbing aerosol plume versus atmospheric molecular radiance multiplied by air mass. We have also plotted for all the viewing geometries of the pixel the computed absorption contribution of aerosol for a dust model (D'Almeida, 1991) and for many vertical structures (i.e. the aerosol altitude). That contribution is computed as follow :

$$\Delta\rho_{abs}(\theta_s, \theta_v, \phi) = \rho_{aer}(\theta_s, \theta_v, \phi) - \rho_{aer}(\theta_s, \theta_v, \phi)(\omega_0=1) \qquad (12)$$

$\rho_{aer}(\theta_s, \theta_v, \phi)$ is the aerosol model reflectance and $\rho_{aer}(\theta_s, \theta_v, \phi)(\omega_0=1)$ is the aerosol model reflectance without absorption (single scattering albedo ω_0 has been forced to 1) at 443 nm, computed using our Successive Order of Scattering code (Deuzé, 1989). We can observed that those parameters are related almost linearly with rayleigh scattering multiplied by air mass. The slope of the linear regression is related to the efficacy of the absorption.

Those characteristics have been implemented in POLDER-2 operational algorithm using aerosol families concept. An aerosol families is a set (12) of models with consistent absorption. The core of the algorithm is played for each families, and the slope defined above is computed for each family. The family that leads to the slope nearest zero is selected for final atmospheric corrections.

Atmospheric correction of Ocean Colour bands (443, 490, 565 and 670 nm)

After the two steps described above have been gone through twice (one iteration) for each family, the aerosol model, optical thickness and family inverted from that process are used to compute surface marine reflectance from TOA normalised radiances.

First and for each viewing direction a *NIR equivalent corrected radiance* (R_e) is computed as a weighted mean for the three red and NIR bands :

$$R_e(i) = \frac{a_{670}R_{corr}(670,i) + a_{765}R_{corr}(765,i) + a_{865}R_{corr}(865,i)}{a_{670} + a_{765} + a_{865}} \tag{13}$$

where a_{670}, a_{765} and a_{865} are the weights accorded to each band. For POLDER-1 and for the noise considerations mention above a_{765}=0 and a_{670}=a_{865}=0.5. Then for each viewing direction and each Ocean Colour bands, radiance spectral dependence is interpolated on five variables (θ_s, θ_v, ϕ, X-disX, τ_a) in LUT defined as :

$$\varepsilon_e(\lambda_j,i) = R_{\text{mod}}(\lambda_j,i)\frac{a_{670} + a_{765} + a_{865}}{a_{670}R_{\text{mod}}(670,i) + a_{765}R_{\text{mod}}(765,i) + a_{865}R_{\text{mod}}(865,i)} \tag{14}$$

When computing the LUT for ε_e, geometric conditions, i.e. the triplet (θ_s, θ_v, ϕ), are supposed identical for each band. But within a POLDER sequences (viewing directions), the different bands are not exactly simultaneous because of the specific design of the POLDER instrument. A fine correction on ε_e correction is then necessary. The correction factor is defined by :

$$\Delta R(\lambda_j,i) = \frac{P(\gamma^{\lambda_j,i})\mu_v^{765,i}}{P(\gamma^{765,i})\mu_v^{\lambda_j,i}} \tag{15}$$

where $P(\gamma^{\lambda_j,i})$ and $P(\gamma^{765,i})$ are the phase function of model X-disX for scattering angle $\gamma^{\lambda,i}$ and $\gamma^{765,i}$ respectively and $\mu_v^{\lambda_j,i}$ and $\mu_v^{765,i}$ are the cosine of view zenith angle of band λ and 765 respectively, for viewing direction i. Band 765 is considered as representative of the three NIR bands (670, 765, 865) used in the atmospheric correction scheme.

The correction term that accounts for aerosol contribution for each Ocean Colour bands (443, 490, 565) can then be easily computed by :

$$R_a(\lambda_j,i) = \varepsilon_e(\lambda_j,i).R_e(\lambda_j,i).\Delta R(\lambda_j,i) \tag{16}$$

The corrected radiance is given by :

$$R_w(\lambda_j,i) = R_{mes}(\lambda_j,i) - R_{mol}(\lambda_j,i) - R_{gm}(\lambda_j,i) - t(\lambda_j,i).R_g - R_a(\lambda_j,i) \tag{17}$$

And finaly the surface marine reflectance for each viewing direction i and each bands j=443, 490 and 565 nm is given by :

$$\rho_w(\lambda_j,i) = \frac{R_w(\lambda_j,i)}{\mu_s.T^{\downarrow\uparrow}(\lambda_j,i) + S(\lambda_j).R_w(\lambda_j,i)} - \rho_f(\lambda_j) \tag{18}$$

Sun-glint correction

For a given POLDER pixel 12 or 13 viewing directions are available. A couple of them are highly contaminated by sun-glint and are then rejected (cf. sun-glint mask). Still some of the directions considered as sun-glint free are slighly contaminated. The correction term for those directions is $t(\lambda).R_g$. R_g is considered spectrally flat and is computed using Cox and Munk model and surface wind-speed from meteorological data. That correction is applied for $R_g < 0.005$. For higher R_g it would not be precise enough (uncertainties on surface wind-speed, intrinsic variability of fresnel reflexion on a rough surface).

Foam correction

When sea-surgace agitation becomes important, generely for important windspeed, air-sea interface can be largely contaminated by whitecaps (Koepke, 1984, Monahan and O'Muircheartaigh, 1986). An empirical relationship between surface density of whitecaps and windspeed has been provided by some of those authors and is widely used :

$$x = 2.95 \times 10^{-6} W^{3.52}$$

where x is the fraction of sea-surface covered by whitecaps and W is the surface windspeed in m/s.
Whitecaps reflectance has been measured in-situ and its mean value is generally considered to be

$$\rho_f = 0.22$$

And more recently other in-situ (Frouin et al., 1997) or air-craft measurements (Moore et al, 2000, Nicolas et al., 2001) have shown that whitecaps reflectance can not be considered as spectrally flat in visible and NIR region. So the model we used for foam reflectance is :

$$\rho_f(\lambda) = \varepsilon_f(\lambda) \,.\, \rho_f \,.\, x$$

where $\varepsilon_f(\lambda)$ are spectral foam coefficient defined for each band from 443 to 865 nm. Surface windspeed used to compute x comes from meteorological data and a threshold on windspeed is set to 8 m/s in order not to compute a foam reflectance for low windspeed.

Last, in the *aerosol optical inversion* module, if $R_{corr}(865) < 0$ and foam reflectance used in equation xxx is not 0 then $\rho_f(\lambda)$ is progressively lowered up until $R_{corr}(865)$ becomes positive. If not, no aerosol correction and no foam correction are made for the pixel (that still can be rejected further in the processing line).

Tables, organigrams and figures

	443 nm	***490 nm***	***565 nm***	***670 nm***	***765 nm***	***865 nm***
$<\tau_r(\lambda)>$	0.23140	0.15270	0.08719	0.04340	0.02572	0.01581

Table 1. Rayleigh optical thickness for each band

	M98	***M95***	***M90***	***M80***	***C90***	***C80***	***C70***	***T99***	***T98***	***T90***	***T80***	***T70***
Angström coeff.	0.110	0.158	0.204	0.209	0.409	0.412	0.674	1.279	1.393	1.528	1.624	1.678
singl. scatt. albedo	0.998	0.997	0.996	0.994	0.994	0.991	0.982	0.992	0.989	0.982	0.972	0.961

Table 2. Aerosol models optical characteristics. M, C and T account for Maritime, Coastal and Tropospheric aerosols respectively. The number is the relative humidity according to the Shettle and Fenn classification

AOT tabulated nodes	0.05	0.10	0.15	0.20	0.30	0.40	0.50	0.70	1.00

Table 3. Aerosol Optical Thickness tabulated nodes used in LUT

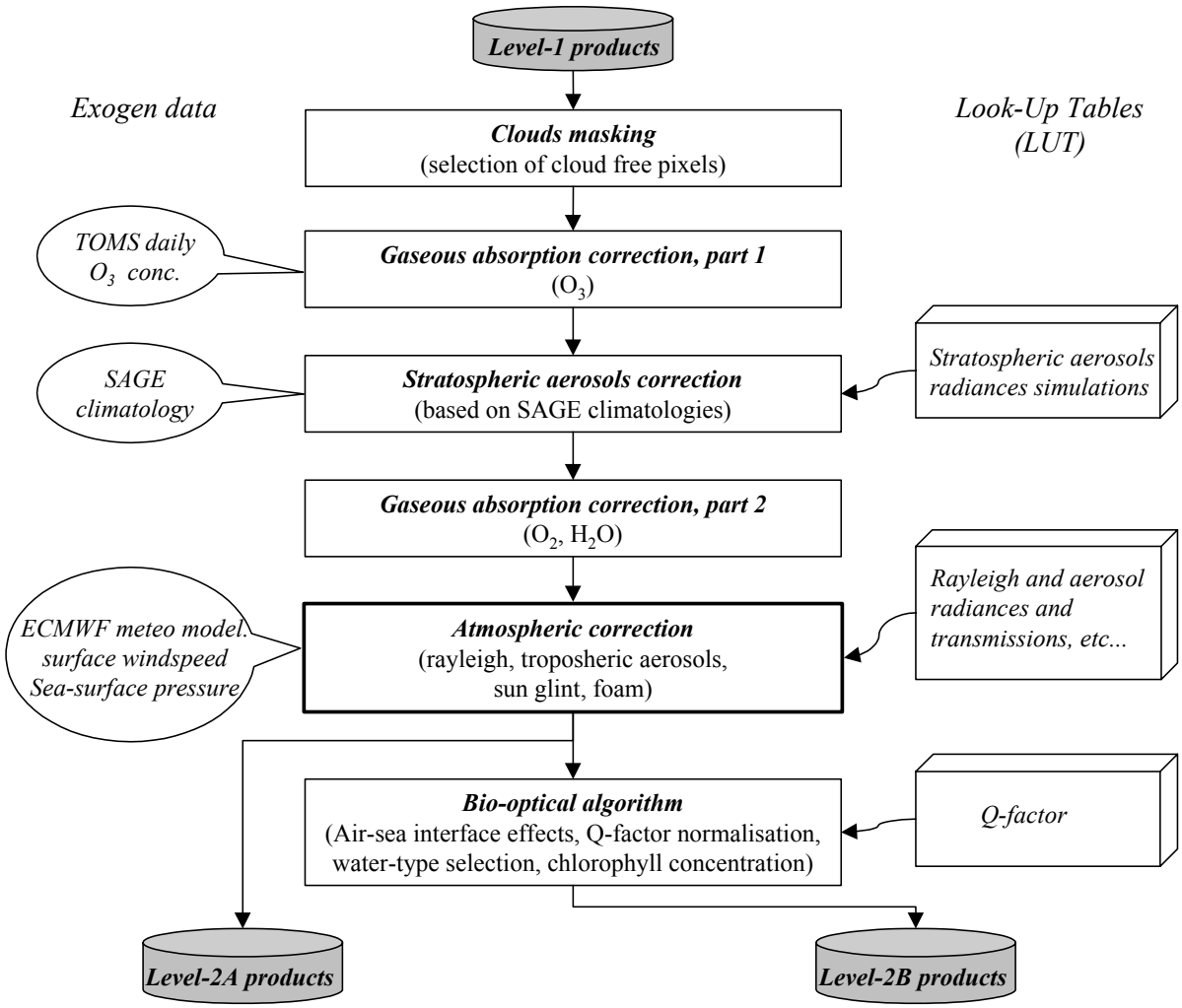

Organigram 1. Complete level-1 to level-2 processing line for POLDER Ocean Color data

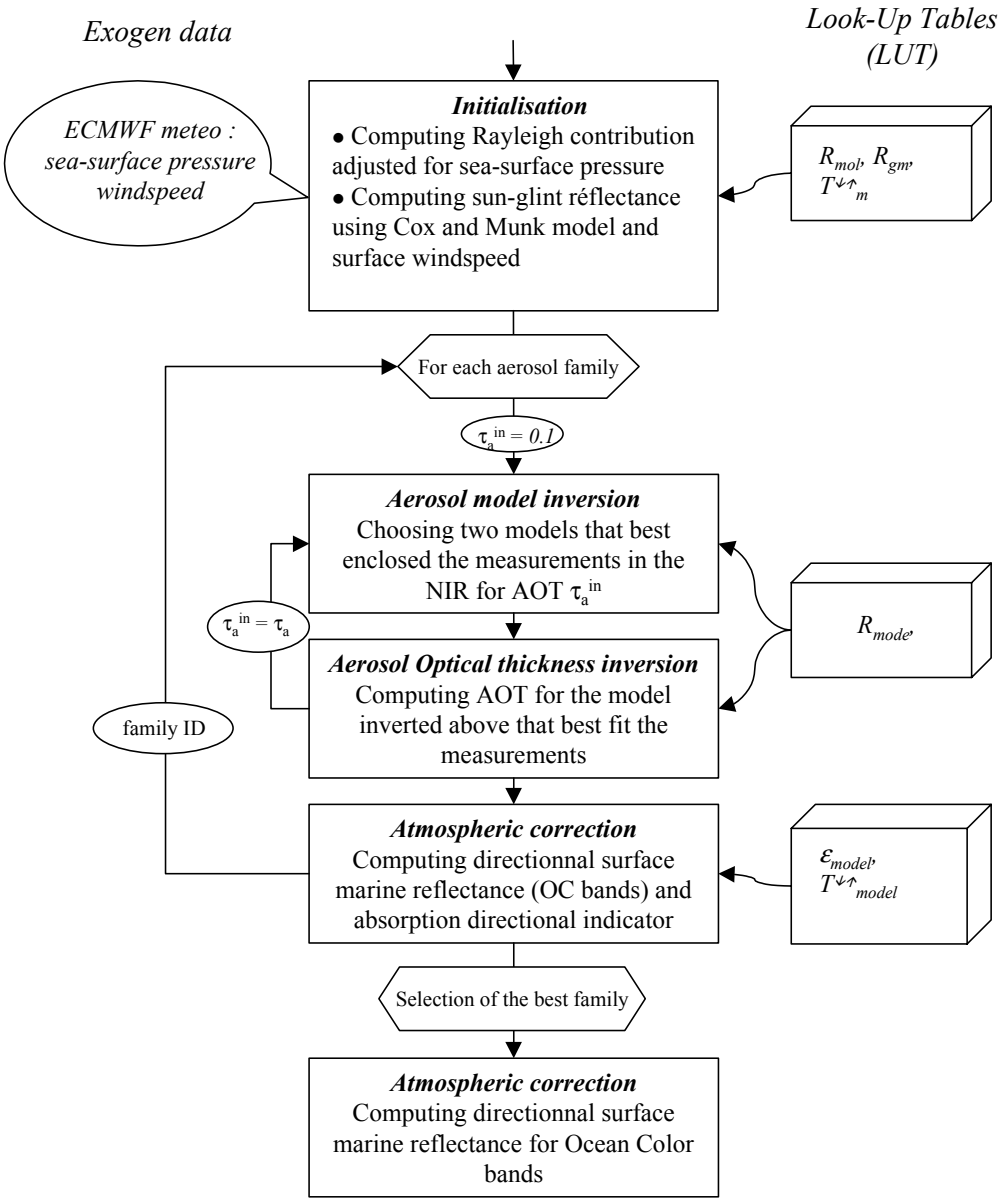

Organigram 2. detailed atmospheric correction algorithm

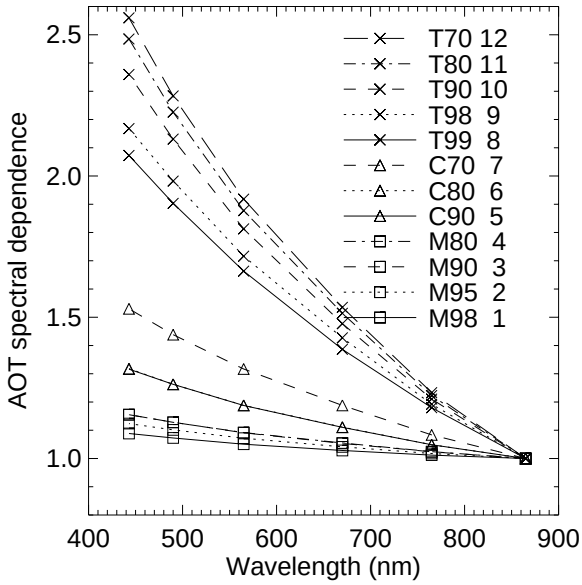

Figure 1 : Spectral dependence of the aerosol optical thickness for the 12 models used in the algorithm

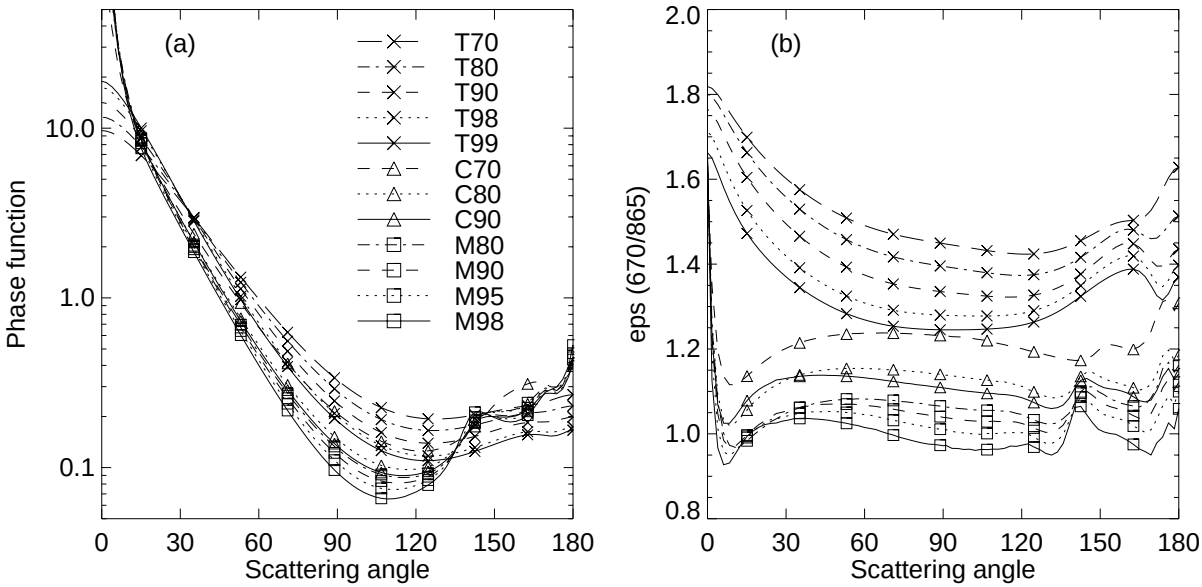

Figure 2 : phase function and single scattering spectral dependence for the 12 models

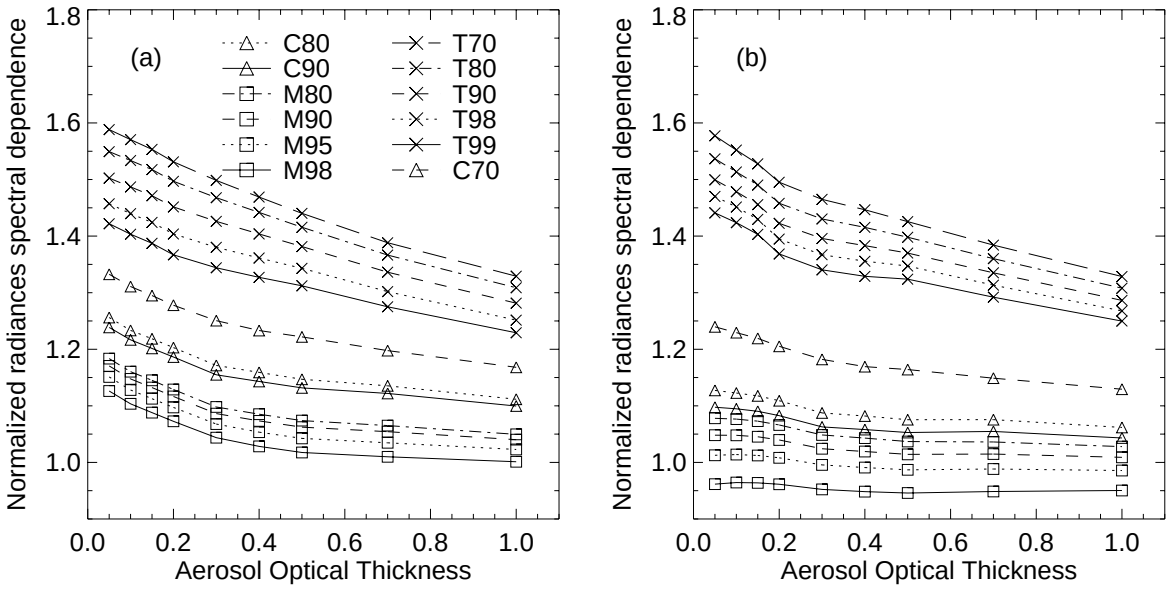

Figure 3 : Spectral dependence of the normalized radiances (including multiple scattering effects) for the 12 models and for 2 geometries : θ_s=60°, θ_v=45°, ϕ=90° or 180°

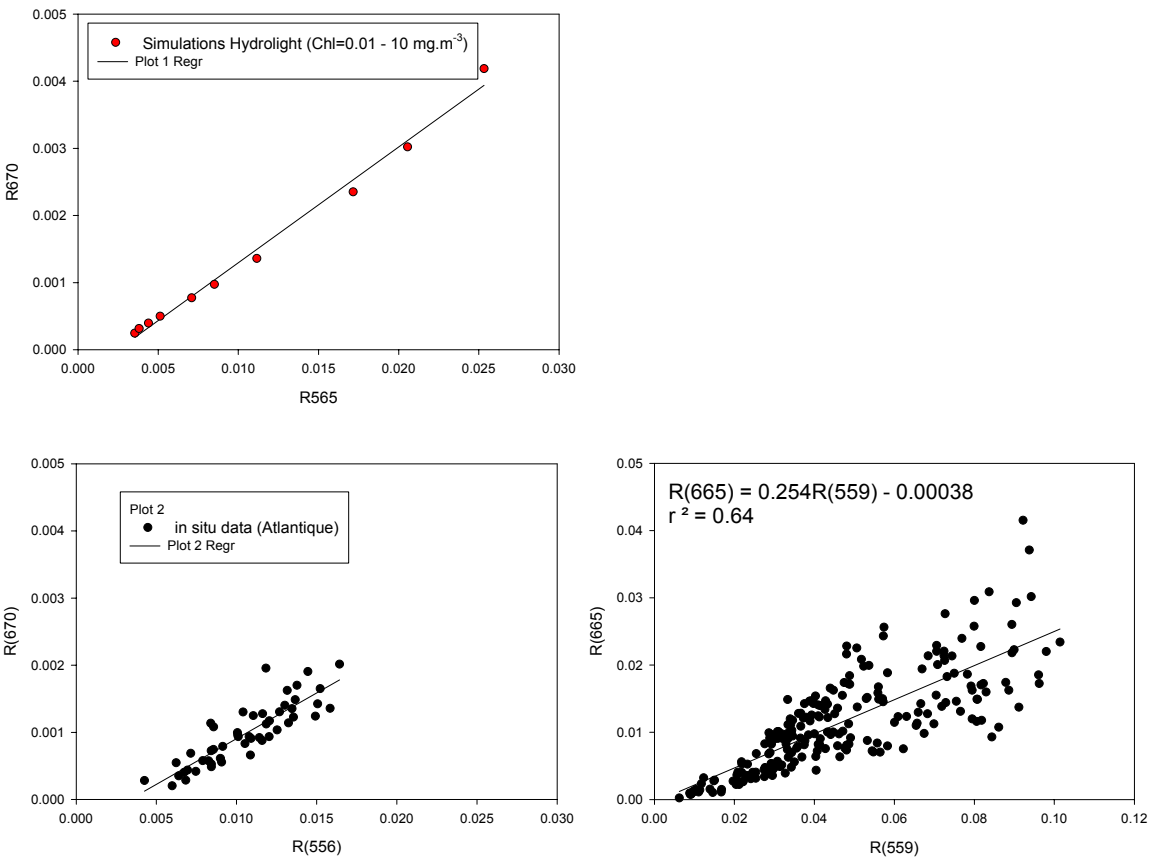

Figure 4. Empirical relationship between marine reflectance at 565 and 670 for case 1 waters (left, simulation and in-situ measurements) and for case 2 waters (right, in-situ measurements during coastlooc)

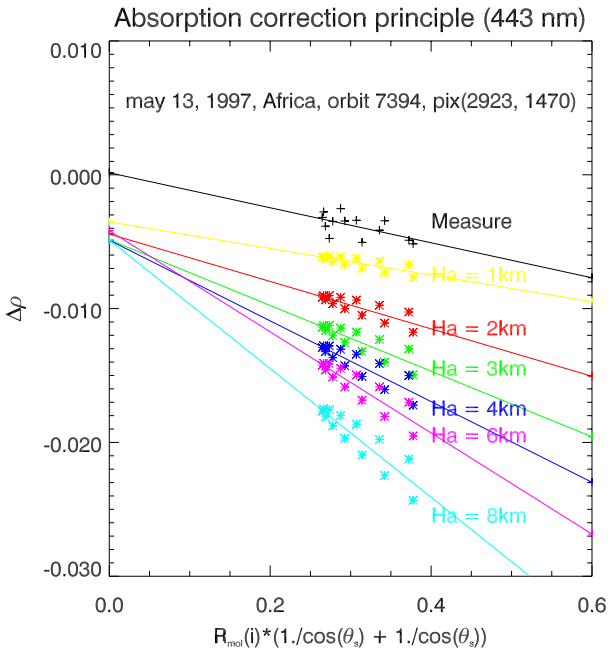

Figure 5 : Illustration of the absorption correction principle for a POLDER pixel over African dust plume in may 1997 (in black) versus simulations (colored) ; it is the slope, and not the absolute level of the signal contaminated by surface reflectance, that should be considered.

References

d'Almeida, G. A., P. Koepke, E. P. Shettle, Atmospheric aerosol - Global Climatology and Radiative Characteristis, *Deepack, Hampton, Va*., 1991

Cox, C. and W. Munk, Measurement of the roughness of the sea surface from photographs of the sun's glitter*, J. Opt. Soc. Am.*, 44, 11, 838-850, 1954

Deuzé, J.-L., M. Herman, R. Santer, Fourier series expansion of the transfer equation in the atmosphere-ocean system, *J. Quant. Spectrosc. Radiat. Transfer*, 41, 483-494, 1989

Frouin, R., M. Schwindling, and P.-Y. Deschamps, Spectral reflectance of sea foam in the visible and near infrared: In-situ measurements and remote sensing implications. *J. Geophys. Res*., 101, 14361-14371, 1996.

Frouin, R., S. F. Iacobellis, and P.-Y. Deschamps, Influence of oceanic whitecaps on the global radiation budget. *Geophys. Res. Lett*., 28, 1523-1526.

Gordon, H. R., and M. Wang, Retrieval of water-leaving radiance and aerosol optical thickness over the oceans with SeaWiFS: A preliminary algorithm, *Appl. Optics*, 33, 443-452, 1994.

Gordon, H. R., T. Du, T. Zhang, Remote sensing of ocean color and aerosol properties : resolving the issue of aerosol absorption, *Appl. Opt*., vol. 36, no. 33, 8670-8684, 1997

Hansen, J. E. and L. D. Travis, Light Scattering in Planetary Atmospheres, *Space Sci. Rev*. **16**, 527 (1974)

Koepke, P., Effective reflectance of oceanic whitecaps, *Appl. Opt*., 23, 1816-1824, 1984

Monahan, E. C., and I. G. O'Muircheartaigh, Optimal power-law description of oceanic whitecap coverage dependence on wind speed, *J. Phys. Oceanogr*., 10, 2094-2099, 1980.

Moore, K. D., K. J. Voss, and H. R. Gordon, Spectral reflectance of whitecaps: Their contribution to water-leaving radiance. *J. Geophys. Res*., 105, 6493-6499, 2000.

Moulin, C. , Gordon H. R. , Chomko R. M. , Banzon V. F. , Evans R. H., Atmospheric correction of ocean color imagery through thick layers of Saharan dust, *Geophys. res. lett*., vol. 28, 5-8, 2001

Nicolas, J.-M., P.-Y. Deschamps, R. Frouin, Spectral reflectance of oceanic whitecaps in the visible and near infrared: Aircraft measurements over open ocean, *Geophys. Res. Lett.*, 28, 23, 4445-4448, 2001

Ruddick, K. G. , Ovidio F. , Rijkeboer M., Atmospheric correction of SeaWiFS imagery for turbid coastal and inland waters, *Appl. opt.* , vol. 39 , no. 6 , 897-912, 2000

Shettle, E. P., and R. W. Fenn, Models for the aerosols of the lower atmosphere and the effects of humidity variations on their optical properties, *AFGL-TR-79-0214*, No 676, 1979

Siegel, D. A. , M. Wang , S. Maritorena. , W. Robinson, Atmospheric correction of satellite ocean color imagery: the black pixel assumption, *Appl. Opt*., vol. 39 , no. 21 , 3582-3591, 2000

Viollier, M., B. Sturm, CZCS data analysis in turbid coastal water, *J. Geophys. Res*., 89, D4, 4977-4985, 1984

Young, A. T., Revised Depolarization Corrections for Atmospheric extinction, *Appl. Opt*., **19**, 3427-3428 (1980)